

Insertion of CO₂, Ketones, and Aldehydes into the C–Li Bond of 1,3,5-Triaza-7-phosphaadamantan-6-yllithium

Gene W. Wong, Wei-Chih Lee, and Brian J. Frost*

Department of Chemistry, MS 216, University of Nevada, Reno, Nevada 89557

Received September 29, 2007

The synthesis and structures of a series of new water-soluble phosphine ligands based on 1,3,5-triaza-7-phosphaadamantane (PTA) are described. Insertion of aldehydes or ketones into the C–Li bond of 1,3,5-triaza-7-phosphaadamantan-6-yllithium (PTA–Li) resulted in the formation of a series of slightly water-soluble β -phosphino alcohols (PTA–CRR'OH, R = C₆H₅, C₆H₄OCH₃, ferrocenyl; R' = H, C₆H₅, C₆H₄OCH₃) derived from the heterocyclic phosphine PTA. Insertion of CO₂ yielded the highly water-soluble carboxylate PTA–CO₂Li, $S_{25}^{\circ} \approx 800$ g/L. The compounds have been fully characterized in the solid state by X-ray crystallography and in solution by multinuclear NMR spectroscopy. The addition of PTA–Li to symmetric ketones results in a racemic mixture of PTA–CR₂OH ligands with a single resonance in the ³¹P{¹H} NMR spectrum between –95 and –97 ppm. The addition of PTA–Li to aldehydes results in a mixture of diastomeric compounds, PTA–CHROH, with two ³¹P{¹H} NMR resonances between –100 and –106 ppm. Three (η^6 -arene)RuCl₂(PTA–CRR'OH) complexes of these ligands were synthesized and characterized, with the ligands binding in a κ^1 coordination mode. All the ligands and ruthenium complexes are slightly soluble in water with $S_{25}^{\circ} = 3.9$ –11.1 g/L for the PTA–CRR'OH ligands and $S_{25}^{\circ} = 3.3$ –14.1 g/L for the (η^6 -arene)RuCl₂(PTA–CRR'OH) complexes.

Introduction

The air-stable, water-soluble, heterocyclic phosphine 1,3,5-triaza-7-phosphaadamantane (PTA) has received a great deal of attention in recent years.^{1,2} This newfound attention has been in part due to reports that ruthenium complexes of PTA

have displayed anticancer properties.^{3–13} Our group has been interested in the coordination chemistry of PTA^{14–18} and its utility as a ligand in catalysis.^{19,20} A handful of PTA

* To whom correspondence should be addressed. E-mail: Frost@unr.edu.

- (1) Phillips, A. D.; Gonsalvi, L.; Romerosa, A.; Vizza, F.; Peruzzini, M. *Coord. Chem. Rev.* **2004**, *248*, 955–993 and references within.
- (2) For example see: (a) Vergara, E.; Miranda, S.; Mohr, F.; Cerrada, E.; Tiekink, E. R. T.; Romero, P.; Mendía, A.; Laguna, M. *Eur. J. Inorg. Chem.* **2007**, 2926–2933. (b) Gossens, C.; Dorcier, A.; Dyson, P. J.; Rothlisberger, U. *Organometallics* **2007**, 3969–3975. (c) Kirillov, A. M.; Smoleňski, P.; Guedes da Silva, M. F. C.; Pombeiro, A. J. L. *Eur. J. Inorg. Chem.* **2007**, 2686–2692. (d) Xu, X.; Wang, C.; Zhou, Z.; Tang, X.; He, Z.; Tang, C. *Eur. J. Org. Chem.* **2007**, 4487–4491. (e) Mohr, F.; Falvello, L. R.; Laguna, M. *Eur. J. Inorg. Chem.* **2006**, 3152–3154. (f) He, Z.; Tang, X.; Chen, Y.; He, Z. *Adv. Synth. Catal.* **2006**, *348*, 413–417. (g) Krogstad, D. A.; Cho, J.; DeBoer, A. J.; Klitzke, J. A.; Sanow, W. R.; Williams, H. A.; Halfen, J. A. *Inorg. Chim. Acta* **2006**, *359*, 136–148. (h) Frost, B. J.; Mebi, C. A. *Organometallics* **2004**, *23*, 5317–5323. (i) Bolaño, S.; Gonsalvi, L.; Zanolini, F.; Vizza, F.; Bertolasi, V.; Romerosa, A.; Peruzzini, M. *J. Mol. Catal. A* **2004**, *224*, 61–70. (j) Dyson, P. J.; Ellis, D. J.; Henderson, W.; Laurency, G. *Adv. Synth. Catal.* **2003**, *345*, 216–221. (k) Smolenski, P.; Pruchnik, F. P.; Ciunik, Z.; Lis, T. *Inorg. Chem.* **2003**, *42*, 3318–3322. (l) Akbayeva, D. N.; Gonsalvi, L.; Oberhauser, W.; Peruzzini, M.; Vizza, F.; Bruggeller, P.; Romerosa, A.; Sava, G.; Bergamo, A. *Chem. Commun.* **2003**, 264–265. (m) Kovács, J.; Todd, T. D.; Reibenspies, J. H.; Joó, F.; Darensbourg, D. J. *Organometallics* **2000**, *19*, 3963–3969.

- (3) Allardyce, C. S.; Dyson, P. J.; Ellis, D. J.; Heath, S. L. *Chem. Commun.* **2001**, 1396–1397.
- (4) Dorcier, A.; Dyson, P. J.; Gossens, C.; Rothlisberger, U.; Scopelliti, R.; Tavernelli, I. *Organometallics* **2005**, *24*, 2114–2123.
- (5) Scolaro, C.; Bergamo, A.; Brescacin, L.; Delfino, R.; Cocchietto, M.; Laurency, G.; Geldbach, T. J.; Sava, G.; Dyson, P. J. *J. Med. Chem.* **2005**, *48*, 4161–4171.
- (6) Dyson, P. J.; Sava, G. *Dalton Trans.* **2006**, 1929–1933.
- (7) Dorcier, A.; Ang, W. H.; Bolaño, S.; Gonsalvi, L.; Juillerat-Jeanerret, L.; Laurency, G.; Peruzzini, M.; Phillips, A. D.; Zanolini, F.; Dyson, P. J. *Organometallics* **2006**, *25*, 4090–4096.
- (8) Scolaro, C.; Geldbach, T. J.; Rochat, S.; Dorcier, A.; Gossens, C.; Bergamo, A.; Cocchietto, M.; Tavernelli, I.; Sava, G.; Rothlisberger, U.; Dyson, P. J. *Organometallics* **2006**, *25*, 756–765.
- (9) Ang, W. H.; Dyson, P. J. *Eur. J. Inorg. Chem.* **2006**, 4003–4018.
- (10) Allardyce, C. S.; Dyson, P. J.; Ellis, D. J.; Salter, P. A.; Scopelliti, R. *J. Organomet. Chem.* **2003**, *668*, 35–42.
- (11) Grguric-Sipka, S.; Kowol, C. R.; Valiahdhi, S.-M.; Eichinger, R.; Jakupec, M. A.; Roller, A.; Shova, S.; Arion, V. B.; Keppler, B. K. *Eur. J. Inorg. Chem.* **2007**, 2870–2878.
- (12) Leyva, L.; Sirlin, C.; Rubio, L.; Franco, C.; Le Lagadec, R.; Spencer, J.; Bischoff, P.; Gaidon, C.; Loeffler, J.-P.; Pfeffer, M. *Eur. J. Inorg. Chem.* **2007**, 3055–3066.
- (13) Casini, A.; Mastrobuoni, G.; Ang, W. H.; Gabbiani, C.; Pieraccini, G.; Moneti, G.; Dyson, P. J.; Messori, L. *ChemMedChem* **2007**, *2*, 631–635.
- (14) Mebi, C. A.; Frost, B. J. *Inorg. Chem.* **2007**, *46*, 7115–7120.
- (15) Mebi, C. A.; Frost, B. J. *Z. Anorg. Allg. Chem.* **2007**, *633*, 368–371.
- (16) Frost, B. J.; Bautista, C. M.; Huang, R.; Shearer, J. *Inorg. Chem.* **2006**, *45*, 3481–3483.

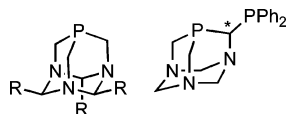
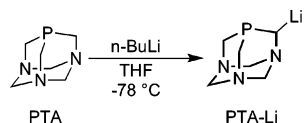


Figure 1. PTA_{R_3} and $\text{PTA}-\text{PPh}_2$.

Scheme 1



derivatives have been published with most of the modifications focused on the “lower rim” PTA; i.e., the triazacyclohexane ring.^{21–26} Cleavage of C–N or C–P bonds has led to a few different “ring-opened” PTA derivatives, which have appeared in the literature over the years.^{27–31} Most recently, we have focused on developing derivatives that maintain the core structure of PTA.^{32,33} We have recently shown that the “lower-rim” of PTA may be trisubstituted, leading to sterically bulky derivatives of PTA (Figure 1).³³ The “lower-rim” PTA derivatives are interesting; however, modification of the triazacyclohexane ring of PTA leads to changes distant from phosphorus and, therefore, any coordinated metal center. Of particular interest are chiral “upper-rim” PTA derivatives where a stereogenic center can be installed at the carbon adjacent to phosphorus.

We have previously reported a method for the synthesis of upper-rim PTA derivatives, in which the first step is lithiation at the α -carbon of PTA (Scheme 1).³² Using $\text{PTA}-\text{Li}$ we synthesized and characterized $\text{PTA}-\text{PPh}_2$ (Figure 1); unfortunately, it was isolated in low yield and insoluble in water.³²

Herein, we report the synthesis and characterization of a series of water-soluble β -phosphino alcohols, $\text{PTA}-\text{CR}-$

$\text{R}'\text{OH}$, and carboxylates, $\text{PTA}-\text{CO}_2\text{Li}$, based on the insertion of electrophiles into the C–Li bond of $\text{PTA}-\text{Li}$.

Experimental Section

Materials and Methods. Unless otherwise noted, all manipulations were performed on a double-manifold Schlenk vacuum line under nitrogen or in a nitrogen-filled glovebox. Tetrahydrofuran (THF) was freshly distilled under nitrogen from sodium/benzophenone. Dichloromethane and chloroform were degassed and dried with activated molecular sieves. Water was distilled and deoxygenated before use. Benzophenone, anisaldehyde, ferrocene carboxaldehyde, and instrument-grade CO_2 were purchased from commercial sources and used as received. NMR solvents and $^{13}\text{C}-\text{CO}_2$ were purchased from Cambridge Isotopes and used as received. Tetrakis(hydroxymethyl)phosphonium chloride was obtained from Cytec and used without further purification. 1,3,5-Triaza-7-phosphaadamantane (PTA),³⁴ $\text{PTA}-\text{Li}$,³² $[(\eta^6-\text{C}_6\text{H}_6)\text{RuCl}_2]_2$,³⁵ and $[(\eta^6-\text{C}_6\text{H}_5\text{CH}_3)\text{RuCl}_2]_2$ ³⁵ were synthesized as reported in the literature. NMR spectra were recorded with Varian Unity Plus 500 FT-NMR or Varian NMR System 400 spectrometers. ^1H and ^{13}C NMR spectra were referenced to residual solvent relative to tetramethylsilane (TMS). Phosphorus chemical shifts are relative to an external reference of 85% H_3PO_4 in D_2O with positive values downfield of the reference. IR spectra were recorded on a Perkin-Elmer 2000 FT-IR spectrometer as KBr pellets. X-ray crystallographic data were collected at $100(\pm 1)$ K on a Bruker APEX CCD diffractometer with $\text{Mo K}\alpha$ radiation ($\lambda = 0.71073$ Å) and a detector-to-crystal distance of 4.94 cm. Data collection was optimized utilizing the APEX 2 software³⁶ with 0.5° rotation between frames. Data integration, correction for Lorentz and polarization effects, and final cell refinement were performed using SAINTPLUS and corrected for absorption using SADABS. The structures were solved by direct methods and refined using SHELXTL, version 6.10.³⁶ Crystallographic data and data collection parameters are listed in Table 1. A complete list of bond lengths and angles may be found in the Supporting Information.

Caution! $\text{PTA}-\text{Li}$ is a highly pyrophoric solid, igniting violently upon exposure to air.

Synthesis of Lithium 1,3,5-Triaza-7-phosphaadamantane-6-carboxylate ($\text{PTA}-\text{CO}_2\text{Li}$). $\text{PTA}-\text{Li}$ (1.23 g, 7.56 mmol) was suspended in 35 mL of dry THF and cooled to -78°C . Dry CO_2 (g) was bubbled into the solution for 2 h at -78°C . The solution was then warmed to room temperature, and CO_2 bubbled through the solution for an additional 2 h. The solvent was removed under vacuum, and the solid washed with CHCl_3 to remove residual PTA, resulting in 1.38 g of an off-white solid (88% yield). ^1H NMR (400 MHz, D_2O): 4.75–4.28 (m, 6H, NCH_2N); 3.95 (m, 1H, PCHN); 3.85–3.6 (m, 4H, PCH_2N). $^{31}\text{P}\{^1\text{H}\}$ NMR (162 MHz, D_2O): -88.0 (s). IR ν_{CO_2} (KBr, cm^{-1}): $\text{PTA}-\text{CO}_2\text{Li}$, 1614 (s, asymmetric stretch) and 1399 (m, symmetric stretch); $\text{PTA}-^{13}\text{CO}_2\text{Li}$, 1592 (s) and 1371 (m).

Synthesis of Methyl-1,3,5-triaza-7-phosphatrimethyl-3,3,1,1,3,7]-decane-6-carboxylate ($\text{PTA}-\text{CO}_2\text{CH}_3$). In a 50 mL Schlenk flask, 1.03 g (4.98 mmol) $\text{PTA}-\text{CO}_2\text{Li}$ was dissolved in 50 mL of

- (17) Frost, B. J.; Mebi, C. A.; Gingrich, P. W. *Eur. J. Inorg. Chem.* **2006**, 1182–1189.
 (18) Frost, B. J.; Miller, S. B.; Rove, K. O.; Pearson, D. M.; Korinek, J. D.; Harkreader, J. L.; Mebi, C. A.; Shearer, J. *Inorg. Chem. Acta* **2006**, 359, 283–288.
 (19) Mebi, C. A.; Nair, R. P.; Frost, B. J. *Organometallics* **2007**, 26, 429–438.
 (20) Mebi, C. A.; Frost, B. J. *Organometallics* **2005**, 24, 2339–2346.
 (21) Navech, J.; Kraemer, R.; Majoral, J. P. *Tetrahedron Lett.* **1980**, 21, 1449–1452.
 (22) Benhammou, M.; Kraemer, R.; Germa, H.; Majoral, J. P.; Navech, J. *Phosphorus Sulfur Relat. Elem.* **1982**, 14, 105–119.
 (23) Daigle, D. J.; Boudreaux, G. J.; Vail, S. L. *J. Chem. Eng. Data* **1976**, 21, 240–241.
 (24) Delerno, J. R.; Majeste, R. J.; Trefonas, L. M. *J. Heterocycl. Chem.* **1976**, 13, 757–760.
 (25) Daigle, D. J.; Pepperman, A. B., Jr.; Boudreaux, G. J. *Heterocycl. Chem.* **1974**, 11, 1085–1086.
 (26) Darenbourg, D. J.; Yarbrough, J. C.; Lewis, S. J. *Organometallics* **2003**, 22, 2050–2056.
 (27) (a) Siele, V. I. *J. Heterocycl. Chem.* **1977**, 14, 337–339. (b) Fluck, E.; Weissgraber, H. *J. Chem.-Ztg.* **1977**, 101, 304.
 (28) (a) Assmann, B.; Angermaier, K.; Paul, M.; Riede, J.; Schmidbaur, H. *Chem. Ber.* **1995**, 128, 891–900. (b) Assmann, B.; Angermaier, K.; Schmidbaur, H. *J. Chem. Soc., Chem. Commun.* **1994**, 941–942.
 (29) Darenbourg, D. J.; Ortiz, C. G.; Kamplain, J. W. *Organometallics* **2004**, 23, 1747–1754.
 (30) Mena-Cruz, A.; Lorenzo-Luis, P.; Romerosa, A.; Saoud, M.; Serrano-Ruiz, M. *Inorg. Chem.* **2007**, 46, 6120–6128.
 (31) Krogstad, D. A.; Ellis, G. S.; Gunderson, A. K.; Hamrlich, A. J.; Rudolf, J. W.; Halfen, J. A. *Polyhedron* **2007**, 26, 4093–4100.
 (32) Wong, G. W.; Harkreader, J. L.; Mebi, C. A.; Frost, B. J. *Inorg. Chem.* **2006**, 45, 6748–6755.
 (33) Huang, R.; Frost, B. J. *Inorg. Chem.* **2007**, 46, 10962–10964.

- (34) (a) Daigle, D. J.; Pepperman, A. B., Jr.; Vail, S. L. *J. Heterocycl. Chem.* **1974**, 11, 407–408. (b) Daigle, D. J. *Inorg. Synth.* **1998**, 32, 40–45.
 (35) Bennett, M. A.; Smith, A. K. *J. Chem. Soc., Dalton. Trans.* **1974**, 233–241.
 (36) Sheldrick, G. M. *SHELXTL: Structure Determination Software Suite*, version 6.10; Bruker AXS: Madison, WI, 2001.

Table 1. Crystallographic Data for O=PTA-CO₂Me, PTA-C(C₆H₅)₂OH, O=PTA-C(C₆H₄OCH₃)₂OH, O=PTA-CH(C₆H₄OCH₃)OH, PTA-CH(ferrocenyl)OH, (η^6 -C₆H₅CH₃)Ru(PTA-C(C₆H₅)₂OH)Cl₂, (η^6 -C₆H₆)Ru(PTA-C(C₆H₄OCH₃)₂OH)Cl₂, and (η^6 -C₆H₆)Ru(PTA-CH(C₆H₄OCH₃)OH)Cl₂

	O=PTA-CO ₂ Me	PTA-C(C ₆ H ₅) ₂ OH	O=PTA-C-(C ₆ H ₄ OCH ₃) ₂ OH	O=PTA-CH-(C ₆ H ₄ OCH ₃)OH
empirical formula	C ₈ H ₁₄ N ₃ O ₃ P	C ₄₀ H ₄₄ N ₆ O ₃ P ₂	C ₂₉ H ₄₂ N ₃ O ₆ P	C ₁₄ H ₂₀ N ₃ O ₃ P
fw	231.19	718.75	559.63	309.30
<i>T</i> (K)	100(2) K	100(2)	100(2)	100(2) K
λ , Å	0.71073	0.71073	0.71073	0.71073
cryst syst	monoclinic	triclinic	triclinic	monoclinic
space group	<i>P</i> 2 ₁ / <i>c</i>	<i>P</i> 1	<i>P</i> 1	<i>P</i> 2 ₁ / <i>c</i>
<i>a</i> (Å)	5.9476(4)	10.1057(4)	11.7005(2)	11.3234(5)
<i>b</i> (Å)	25.4104(18)	10.4672(4)	11.7013(2)	11.3340(4)
<i>c</i> (Å)	7.1910(5)	17.5115(6)	12.9305(2)	11.0327(4)
α (deg)	90	102.716(2)	63.3210(10)	90
β (deg)	112.581(3)	98.658(2)	82.1920(10)	92.691(2)
γ (deg)	90	99.068(2)	62.5270(10)	90
<i>V</i> (Å ³)	1003.47(12)	1751.02(11)	1397.78(4)	1414.37(9)
<i>Z</i>	4	2	2	4
<i>D</i> _{calc} (Mg/m ³)	1.530	1.363	1.330	1.453
abs coeff (mm ⁻¹)	0.266	0.174	0.146	0.209
cryst size (mm ³)	0.18 × 0.07 × 0.03	0.17 × 0.07 × 0.03	0.19 × 0.19 × 0.06	0.28 × 0.08 × 0.03
θ for data collect (deg)	1.60 to 25.25	1.21 to 23.50	1.77 to 25.50	1.80 to 25.50
index ranges	-7 ≤ <i>h</i> ≤ 7 -18 ≤ <i>k</i> ≤ 30 -8 ≤ <i>l</i> ≤ 8	-11 ≤ <i>h</i> ≤ 11 -11 ≤ <i>k</i> ≤ 11 -19 ≤ <i>l</i> ≤ 19	-12 ≤ <i>h</i> ≤ 14 -13 ≤ <i>k</i> ≤ 14 -15 ≤ <i>l</i> ≤ 15	-13 ≤ <i>h</i> ≤ 13 -13 ≤ <i>k</i> ≤ 13 -13 ≤ <i>l</i> ≤ 13
reflns collected	8889	15 978	22 924	21 738
indep reflns	1814	5172	5079	2638
abs correction	[<i>R</i> (int) = 0.0810]	[<i>R</i> (int) = 0.0833]	[<i>R</i> (int) = 0.0313]	[<i>R</i> (int) = 0.1403]
data/rest/params	SADABS 1814/0/136	SADABS 5172/0/470	SADABS 5079/0/354	SADABS 2638/0/190
GOF <i>F</i> ²	1.053	1.043	1.051	1.050
final <i>R</i> indices	<i>R</i> 1 = 0.0593	<i>R</i> 1 = 0.0654	<i>R</i> 1 = 0.0432	<i>R</i> 1 = 0.0694
[<i>I</i> > 2 σ (<i>I</i>)]	w <i>R</i> 2 = 0.1472	w <i>R</i> 2 = 0.1482	w <i>R</i> 2 = 0.1089	w <i>R</i> 2 = 0.1192
<i>R</i> indices (all data)	<i>R</i> 1 = 0.1064	<i>R</i> 1 = 0.1138	<i>R</i> 1 = 0.0578	<i>R</i> 1 = 0.1168
CCDC no.	w <i>R</i> 2 = 0.1640 662202	w <i>R</i> 2 = 0.1679 662207	w <i>R</i> 2 = 0.1154 662205	w <i>R</i> 2 = 0.1331 662203

	PTA-CH(ferrocenyl)OH	(η^6 -C ₆ H ₅ CH ₃)Ru(PTA-C-(C ₆ H ₅) ₂ OH)Cl ₂	(η^6 -C ₆ H ₆)Ru(PTA-C-(C ₆ H ₄ OCH ₃) ₂ OH)Cl ₂	(η^6 -C ₆ H ₆)Ru(PTA-CH-(C ₆ H ₄ OCH ₃)OH)Cl ₂
empirical formula	C ₁₇ H ₂₂ FeN ₃ O ₃ P	C ₂₆ H ₃₀ Cl ₂ N ₃ OPRu	C _{27.50} H _{32.50} Cl _{3.50} N ₃ -O ₃ PRu	C _{21.50} H ₂₆ Cl _{6.50} N ₃ -O ₂ PRu
fw	371.20	603.47	709.18	720.92
<i>T</i> (K)	100(2)	100(2)	100(2)	100(2)
λ , Å	0.71073	0.71073	0.71073	0.71073
cryst syst	orthorhombic	monoclinic	monoclinic	triclinic
space group	<i>Pca</i> 2(1)	<i>p</i> 2 ₁ / <i>c</i>	<i>P</i> 2(1>/ <i>c</i>)	<i>P</i> 1
<i>a</i> (Å)	14.4830(8)	9.7656(3)	13.5213(3)	3.1047(4)
<i>b</i> (Å)	5.9165(4)	20.5066(7)	26.9050(5)	14.6644(4)
<i>c</i> (Å)	18.3195(9)	12.6430(4)	16.3829(3)	15.7220(5)
α (deg)	90	90	90	66.1460(10)
β (deg)	90	95.3640(10)	101.3200(10)	87.2920(10)
γ (deg)	90	90	90	82.3810(10)
<i>V</i> (Å ³)	1569.77(16)	2520.79(14)	5844.0(2)	2738.79(14)
<i>Z</i>	4	4	8	4
<i>D</i> _{calc} (Mg/m ³)	1.571	1.590	1.612	1.748
abs coeff (mm ⁻¹)	1.070	0.923	0.947	1.292
cryst size (mm ³)	0.06 × 0.05 × 0.05	0.17 × 0.08 × 0.04	0.14 × 0.11 × 0.03	0.15 × 0.13 × 0.08
θ for data collect (deg)	2.22 to 25.49	1.90 to 23.55	1.48 to 26.00	1.42 to 26.00
index ranges	-17 ≤ <i>h</i> ≤ 14 -7 ≤ <i>k</i> ≤ 7 -22 ≤ <i>l</i> ≤ 22	-10 ≤ <i>h</i> ≤ 10 -22 ≤ <i>k</i> ≤ 23 -14 ≤ <i>l</i> ≤ 14	-16 ≤ <i>h</i> ≤ 16 -33 ≤ <i>k</i> ≤ 33 -20 ≤ <i>l</i> ≤ 20	-16 ≤ <i>h</i> ≤ 15 -18 ≤ <i>k</i> ≤ 18 -19 ≤ <i>l</i> ≤ 19
reflns collected	18 952	18 722	99 182	40 011
indep reflns	2923	3737	11 496	10 766
abs correction	[<i>R</i> (int) = 0.1787]	[<i>R</i> (int) = 0.0764]	[<i>R</i> (int) = 0.0767]	[<i>R</i> (int) = 0.0683]
data/rest/params	SADABS 2923/1/212	SADABS 3737/0/311	SADABS 11496/0/711	SADABS 10766/0/676
GOF <i>F</i> ²	1.028	1.014	1.067	1.093
final <i>R</i> indices	<i>R</i> 1 = 0.0616	<i>R</i> 1 = 0.0360	<i>R</i> 1 = 0.0467	<i>R</i> 1 = 0.0552
[<i>I</i> > 2 σ (<i>I</i>)]	w <i>R</i> 2 = 0.0831	w <i>R</i> 2 = 0.0689	w <i>R</i> 2 = 0.0961	w <i>R</i> 2 = 0.1341
<i>R</i> indices (all data)	<i>R</i> 1 = 0.1014	<i>R</i> 1 = 0.0603	<i>R</i> 1 = 0.0689	<i>R</i> 1 = 0.0909
CCDC no.	w <i>R</i> 2 = 0.0933 662201	w <i>R</i> 2 = 0.0784 662206	w <i>R</i> 2 = 0.1028 662208	w <i>R</i> 2 = 0.1491 662204

methanol, resulting in a homogeneous yellow solution. Trimethylsilyl chloride (1.70 g, 15.65 mmol) was added dropwise over the course of 15 min, resulting in a white precipitate. The reaction was

stirred overnight at room temperature, and 4 mL of triethylamine was added, resulting in a clear yellow solution. The solvent was removed under reduced pressure, and the residue dissolved in 80

mL of CH_2Cl_2 . The solution was filtered through Celite, and the solvent removed under reduced pressure. The resulting solid was extracted with 6×50 mL diethyl ether. Removal of the Et_2O yielded 506 mg of $\text{PTA}-\text{CO}_2\text{CH}_3$ as a white solid (47% isolated yield). Anal. Calcd For $\text{C}_8\text{H}_{14}\text{O}_2\text{N}_3\text{P}$: C, 44.65; H, 6.56; N, 19.53. Found: C, 44.31; H, 6.51; N, 19.34. ^1H NMR (400 MHz, CDCl_3): 4.88, 4.70 (AB quartet, $J = 14$ Hz, 1H, PCHN); 4.62 (s, 2H, NCH_2N); 4.38–4.53 (m, 4H, NCH_2N); 3.78–4.10 (m, 4H, PCH_2N); 3.76 (s, 3H, OCH_3). $^{13}\text{C}\{^1\text{H}\}$ NMR (100 MHz, CDCl_3): 170.3 (d, $^2J_{\text{PC}} = 8.9$ Hz, $\text{C}=\text{O}$); 74.6 (s, NCH_2N); 72.5 (d, $^3J_{\text{PC}} = 2.2$ Hz, NCH_2N); 67.9 (d, $^3J_{\text{PC}} = 3.0$ Hz, NCH_2N); 60.1 (d, $^1J_{\text{PC}} = 25.4$ Hz, PCHC); 51.5 (s, OCH_3); 50.2 (d, $^1J_{\text{PC}} = 21.6$ Hz, PCH_2N); 47.2 (d, $^1J_{\text{PC}} = 24.6$ Hz, PCH_2N). $^{31}\text{P}\{^1\text{H}\}$ NMR (162 MHz, CDCl_3): -93.7 (s). IR $\nu_{\text{C}=\text{O}}$ (KBr): 1729 cm^{-1} . X-ray-quality crystals of $\text{O}=\text{PTA}-\text{CO}_2\text{CH}_3$ were obtained over the course of a week by layering a THF solution of $\text{PTA}-\text{CO}_2\text{CH}_3$ with hexanes.

Synthesis of Diphenyl(1,3,5-triaza-7-phosphatricyclo[3.3.1.1^{3,7}]dec-6-yl)methanol ($\text{PTA}-\text{C}(\text{C}_6\text{H}_5)_2\text{OH}$). Benzophenone (2.20 g, 12.1 mmol) was dissolved in 40 mL THF and placed in a slush bath at -78°C (dry ice/acetone). This solution was transferred cold to a Schlenk flask containing 2.00 g (12.2 mmol) lithiated PTA, resulting in a tan suspension. The mixture was stirred at -78°C for 15 min, after which time the reaction was allowed to warm to room temperature. After stirring for 1 h, a white solid was observed precipitating from the yellow solution. Following 2 h of stirring, 0.5 mL water was added to quench the reaction, resulting in a yellow suspension. The solvent was removed under reduced pressure, and the yellow solid washed with a 1:1 mixture of water/acetone resulting in isolation of 3.0 g (73% yield) of an off-white solid. Further purification may be performed by dissolving $\text{PTA}-\text{C}(\text{C}_6\text{H}_5)_2\text{OH}$ in a minimum of warm degassed toluene and storing at $\sim 0^\circ\text{C}$ overnight, resulting in the isolation of a white crystalline analytically pure solid. Anal. Calcd For $\text{C}_{19}\text{H}_{22}\text{O}_1\text{N}_3\text{P}$: C, 67.24; H, 6.53; N, 12.38. Found: C, 66.98; H, 6.48; N, 12.31. ^1H NMR (400 MHz, CDCl_3): 7.65 (d, $J = 7.0$ Hz, 2H, Ar); 7.57 (d, $J = 7.5$ Hz, 2H, Ar); 7.2–7.4 (m, 6H, Ar); 5.33 (s, 1H, PCHN); 4.78 (d, $J = 13.0$ Hz, 1H, NCH_2N); 4.4–4.6 (m, 3H, NCH_2N); 4.34 (d, $J = 13.0$ Hz, 1H, NCH_2N); 4.17 (d, $J = 13.0$ Hz, 1H, PCH_2N); 4.08 (at, $J = 14$ Hz, 1H, PCH_2N); 3.95 (m, 1H, PCH_2N); 3.52 (at, $J = 14$ Hz, 1H, PCH_2N); 3.12 (m, 1H, PCH_2N); 2.35 (s, 1H, OH). $^{13}\text{C}\{^1\text{H}\}$ NMR (100 MHz, CD_2Cl_2): 147.7 (s, Ar); 145.8 (s, Ar); 128.2 (d, $J_{\text{PC}} = 4.6$ Hz, Ar); 127.3 (s, Ar); 127.0 (s, Ar); 126.9 (d, $J_{\text{PC}} = 5.5$ Hz, Ar); 126.3 (d, $J_{\text{PC}} = 5.7$ Hz, Ar); 78.5 (s, $\text{N}-\text{CH}_2-\text{N}$); 78.4 (d, $J_{\text{PC}} = 7.0$ Hz, $\text{C}-\text{C}(\text{C}_6\text{H}_5)_2\text{OH}$); 74.3 (d, $J_{\text{PC}} = 1.9$ Hz, NCH_2N); 66.9 (d, $J_{\text{PC}} = 2.8$ Hz, NCH_2N); 66.0 (d, $J_{\text{PC}} = 27.5$ Hz, $\text{PCHC}(\text{C}_6\text{H}_5)_2\text{OH}$); 52.2 (d, $J_{\text{PC}} = 20.0$ Hz, PCH_2N); 47.4 (d, $J_{\text{PC}} = 25.1$ Hz, PCH_2N). $^{31}\text{P}\{^1\text{H}\}$ NMR (162 MHz, CDCl_3): -95.5 (s). Crystals suitable for X-ray diffraction were obtained by the slow diffusion of pentane into a THF solution of $\text{PTA}-\text{C}(\text{C}_6\text{H}_5)_2\text{OH}$ under nitrogen, resulting in colorless plates over the course of a few days.

Synthesis of Bis-4-methoxyphenyl-(1,3,5-triaza-7-phosphatricyclo[3.3.1.1^{3,7}]dec-6-yl)methanol ($\text{PTA}-\text{C}(\text{C}_6\text{H}_4\text{OCH}_3)_2\text{OH}$). $\text{PTA}-\text{C}(\text{C}_6\text{H}_4\text{OCH}_3)_2\text{OH}$ was synthesized in a manner analogous to that for $\text{PTA}-\text{C}(\text{C}_6\text{H}_5)_2\text{OH}$, resulting in an off-white solid in 62% yield. ^1H NMR (400 MHz, CDCl_3): 7.52 (d, $J = 9$ Hz, 2H, Ar); 7.45 (d, $J = 8$ Hz, 2H, Ar); 6.84 (m, 4H, Ar); 5.15 (s, 1H, OH); 4.78, 4.35 (AB quartet, $J = 12.8$ Hz, 2H, NCH_2N); 4.4–4.6 (m, 4H, NCH_2N); 4.17 (d, $J = 13.6$ Hz, 1H, PCHN); 4.07 (d, $J = 12.8$ Hz, 1H, PCH_2N); 3.88 (m, 1H, PCH_2N); 3.77 (s, 6H, OCH_3); 3.54 (at, $J = 14.8$ and 12.8 Hz 1H, PCH_2N); 3.23 (m, 1H, PCH_2N). $^{31}\text{P}\{^1\text{H}\}$ NMR (162 MHz, CDCl_3): -96.4 (s).

X-ray-quality crystals of $\text{O}=\text{PTA}-\text{C}(\text{C}_6\text{H}_4\text{OCH}_3)_2\text{OH}$ were obtained by layering a THF solution of $\text{PTA}-\text{C}(\text{C}_6\text{H}_4\text{OCH}_3)_2\text{OH}$ with hexanes, resulting in colorless blocks over the course of 3 days.

Synthesis of 4-Methoxyphenyl-(1,3,5-triaza-7-phosphatricyclo[3.3.1.1^{3,7}]dec-6-yl)methanol ($\text{PTA}-\text{CH}(\text{C}_6\text{H}_4\text{OCH}_3)\text{OH}$). *p*-Anisaldehyde (0.84 g, 6.1 mmol) was slowly added via cannula to a cold (-78°C) suspension of 15 mL THF and 1.0 g (6.1 mmol) $\text{PTA}-\text{Li}$. The yellow-white suspension was stirred at -78°C for 15 min and warmed to room temperature after which time the suspension was stirred under nitrogen for 12 h. Water was slowly added until the suspension temporarily cleared. After a few minutes, a white precipitate was observed and the solvent was removed under reduced pressure. The resultant white solid was washed with 50 mL of acetone yielding 1.13 g (63% isolated yield) of the diastereomeric product in a ratio of $\sim 2.5:1$ RS/SR:RR/SS. ^1H NMR of RS/SR diastereomer (400 MHz, CDCl_3): 7.39 (d, $J = 8.8$ Hz, Ar); 6.90 (dd, $J = 6.4$ and 2.0 Hz, Ar); 5.33 (dd, $J = 8.4$ and 5.2 Hz, 1H, $\text{PCHCH}(\text{C}_6\text{H}_4\text{OCH}_3)\text{OH}$); 3.5–5.0 (m, 11H, PCH_2N and NCH_2N). $^{13}\text{C}\{^1\text{H}\}$ NMR of RS/SR diastereomer (100 MHz, $\text{DMSO}-d_6$): 158.9 (s, Ar); 137.7 (s, Ar); 128.3 (s, Ar); 113.8 (s, Ar); 76.5 (s, NCH_2N); 76.1 (s, NCH_2N); 74.1 (d, $^3J_{\text{PC}} = 3$ Hz, NCH_2N); 67.8 (d, $^2J_{\text{PC}} = 4$ Hz, $^*\text{CHOH}$); 66.2 (d, $J_{\text{PC}} = 22$ Hz, P^*CN); 55.7 (s, $-\text{OCH}_3$); 51.2 (d, 20 Hz, PCN); 48.3 (d, 24 Hz, PCN). $^{31}\text{P}\{^1\text{H}\}$ NMR (162 MHz, CDCl_3): -102.6 (s, RS/SR diastereomer), -105.7 (s, RR/SS diastereomer). Colorless X-ray-quality plates of $\text{O}=\text{PTA}-\text{CH}(\text{C}_6\text{H}_4\text{OCH}_3)\text{OH}$ were obtained over the course of a week by layering a CH_2Cl_2 solution of $\text{PTA}-\text{CH}(\text{C}_6\text{H}_4\text{OCH}_3)\text{OH}$ with diethyl ether at 10°C .

Synthesis of $\text{PTA}-\text{CH}(\text{ferrocenyl})\text{OH}$. Ferrocene carboxaldehyde (650 mg, 3.0 mmol) was dissolved in 25 mL of THF and transferred by cannula to a Schlenk flask charged with 510 mg (3.1 mmol) of $\text{PTA}-\text{Li}$ at -78°C . Upon addition, the appearance of an orange precipitate was observed. After stirring for 1.5 h at -78°C , the reaction was allowed to warm to room temperature and stirred overnight (~ 10 h). Water (~ 0.5 mL) was added dropwise until the solution became clear red. The solvent was removed under reduced pressure, and the solid was washed with diethyl ether (3×15 mL), resulting in 790 mg of a red-orange powder (70% yield) isolated as a mixture of diastereomers in a ratio of $\sim 1.8:1$ RS/SR:RR/SS. ^1H NMR (400 MHz, CDCl_3): 5.03 (dt, $J = 13.6$ and 2.4 Hz, 1H, PCHN RS/SR); 4.88 (m, 2H, C_5H_4 RS/SR); 4.80 (dd, $J = 13.2$ and 1.6 Hz, 1H, PCHN RR/SS); 4.71 (m, 2H, C_5H_4 RS/SR); 4.60–4.48 (m, 4H, C_5H_4 RR/SS); 4.47–4.36 (m, NCH_2N RS/SR and RR/SS); 4.32–4.20 (m, NCH_2N RS/SR and RR/SS); 4.22–3.95 (m, PCH_2N RS/SR and RR/SS); 4.26 (s, 5H, Cp SS/RR); 4.23 (s, 5H, Cp SR/RS). $^{31}\text{P}\{^1\text{H}\}$ NMR (162 MHz, CDCl_3): -100.6 (s, major RS/SR), -103.1 (s, minor SS/RR). ESI-MS: 370.2 (M^-). Orange X-ray-quality crystals were obtained as blocks by the slow evaporation of a diethyl ether solution of $\text{PTA}-\text{CH}(\text{ferrocenyl})\text{OH}$.

General Synthesis of $\text{O}=\text{PTA}-\text{CRR}'\text{OH}$. The phosphine oxides $\text{O}=\text{PTA}-\text{CRR}'\text{OH}$ and $\text{O}=\text{PTA}-\text{CO}_2\text{Li}$ were obtained quantitatively by the addition of 30% H_2O_2 (0.2 mmol) to a 1 mL D_2O solution of $\text{PTA}-\text{CRR}'\text{OH}$ or $\text{PTA}-\text{CO}_2\text{Li}$ (0.1 mmol). $^{31}\text{P}\{^1\text{H}\}$ NMR (162 MHz, D_2O): -2.27 (s), $\text{O}=\text{PTA}-\text{CO}_2\text{Li}$; -2.88 (s), $\text{O}=\text{PTA}-\text{CO}_2\text{CH}_3$; 3.97 (s), $\text{O}=\text{PTA}-\text{C}(\text{C}_6\text{H}_5)_2\text{OH}$; 4.14 (s), $\text{O}=\text{PTA}-\text{C}(\text{C}_6\text{H}_4\text{OCH}_3)_2\text{OH}$; 1.72 (s), 2.74 (s), $\text{O}=\text{PTA}-\text{CH}(\text{C}_6\text{H}_4\text{OCH}_3)\text{OH}$; 1.75 (s), 2.82 (s), $\text{O}=\text{PTA}-\text{CH}(\text{ferrocenyl})\text{OH}$. $^{31}\text{P}\{^1\text{H}\}$ NMR (162 MHz, CDCl_3): -0.91 (s), $\text{O}=\text{PTA}-\text{CO}_2\text{Li}$; -11.0 (s), $\text{O}=\text{PTA}-\text{CO}_2\text{CH}_3$; -3.46 (s), $\text{O}=\text{PTA}-\text{C}(\text{C}_6\text{H}_5)_2\text{OH}$; -3.1 (s), $\text{O}=\text{PTA}-\text{C}(\text{C}_6\text{H}_4\text{OCH}_3)_2\text{OH}$; -1.48 (s), -3.19 (s),

O=PTA-CH(C₆H₄OCH₃)OH; -0.06 (s), -1.35 (s), O= PTA-CH(ferrocenyl)OH.

Synthesis of [(η^6 -C₆H₅CH₃)RuCl₂(PTA-C(C₆H₅)₂OH)]. A 50 mL Schlenk flask was charged with 68 mg (0.2 mmol) PTA-C(C₆H₅)₂OH and 53 mg (0.1 mmol) [Ru(η^6 -C₆H₅CH₃)Cl₂]₂ and placed under nitrogen. Dichloromethane (10 mL) was added, and the solution stirred for 15 min and filtered. The solvent was removed under vacuum, yielding 102 mg of an orange solid (85% yield). ¹H NMR (400 MHz, CDCl₃): 7.91 (d, *J* = 7.6 Hz, 2H, Ar); 7.56 (d, *J* = 7.6 Hz, 2H, Ar); 7.40 (t, *J* = 7.5 Hz, 2H, Ar); 7.21 (m, 4H, Ar); 7.08 (t, *J* = 7.4 Hz, 2H, Ar); 5.47 (s, 1H, PCHN); 5.7–5.0 (m, 4H, Ar); 4.1–4.9 (m, 9H, NCH₂N and PCH₂N and Ar); 3.79 (d, *J* = 13.6 Hz, 1H, PCH₂N); 3.68 (d, *J* = 5.6 Hz, 1H, PCH₂N). ³¹P{¹H} NMR (162 MHz, CDCl₃): -31.0 (s). Orange-red X-ray-quality plates were obtained by layering a chloroform solution with hexanes under nitrogen.

Synthesis of [(η^6 -C₆H₆)RuCl₂(PTA-C(C₆H₄OCH₃)₂OH)]. Dry degassed CH₂Cl₂ (40 mL) was added to a 50 mL Schlenk flask charged with [(η^6 -C₆H₆)RuCl₂]₂ (192 mg, 0.38 mmol) and PTA-C(C₆H₄OCH₃)₂OH (307 mg, 0.77 mmol). The suspension was stirred under nitrogen for 1 h, resulting in a clear red solution. The solution was filtered, and the solvent was removed under reduced pressure yielding 405 mg of a red-orange powder (81% isolated yield). Anal. Calcd for C₂₇H₃₂O₃N₃PCl₂Ru: C, 49.93; H, 4.97; N, 6.47. Found: C, 48.87; H, 4.85; N, 6.23. ¹H NMR (400 MHz, CDCl₃): 7.76 (d, *J* = 8.8 Hz, 2H, Ar); 7.43 (d, *J* = 8.8 Hz, 2H, Ar); 6.93 (d, *J* = 8.4 Hz, 2H, Ar); 6.74 (d, *J* = 8.8 Hz, 2H, Ar); 5.60 (br s, 1H, OH); 5.32 (s, 1H, PCHN); 5.08 (s, 6H, C₆H₆); 4.9–4.2 (m, 10H, PCH₂N and NCH₂N); 3.76 (s, 3H, OCH₃); 3.73 (s, 3H, OCH₃). ³¹P{¹H} NMR (162 MHz, CDCl₃): -31.3 (s). Orange-red X-ray-quality plates were obtained by layering a CHCl₃ solution of the complex with pentane under nitrogen.

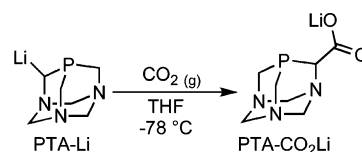
Synthesis of [(η^6 -C₆H₆)RuCl₂(PTA-CH(C₆H₄OCH₃)OH)]. In a 50 mL Schlenk flask containing 101 mg (0.2 mmol) of [(η^6 -C₆H₆)RuCl₂]₂, 118 mg (0.4 mmol) of PTA-CH(C₆H₄OCH₃)OH was placed under nitrogen. Upon addition of methylene chloride (20 mL), all of the phosphine ligand dissolved while some of the ruthenium complex remained suspended in the brown solution. After stirring at room temperature for 4 h, most of the brown solid dissolved. The solution was filtered, and the solvent was removed under reduced pressure resulting in isolation of 182 mg of brown solid (84% yield). ¹H NMR (400 MHz, CDCl₃): 7.35 (d, *J* = 8 Hz, 2H, Ar); 6.93 (d, *J* = 6 Hz, 2H, Ar); 5.71 (s, 1H, PCHN); 5.65 (s, 6H, C₆H₆); 5.42 (s, 1H); (4.7–4.1 (m, 10H, PCH₂N and NCH₂N); 3.81 (s, 3H, OCH₃). ³¹P{¹H} NMR (162 MHz, CD₂Cl₂): -33.12 (s, major diastereomer); -32.33 (s, minor diastereomer). X-ray-quality crystals were obtained as orange blocks by the slow evaporation of a CHCl₃ solution of the complex.

Results and Discussion

We have previously described the synthesis of PTA-Li and its reaction with ClPPH₂ resulting in PTA-PPh₂.³² While this work demonstrated that “upper-rim” PTA derivatives are accessible, we were discouraged that the yield of PTA-PPh₂ was low and the ligand was not soluble in water. In an attempt to increase both the yield and the water solubility, we have explored the reaction of PTA-Li with a variety of electrophiles: namely, CO₂, ketones, and aldehydes.

Insertion of CO₂. Insertion of CO₂ into the C-Li bond of PTA-Li proceeds in high yield, >85%, by bubbling CO₂ through a THF suspension of PTA-Li at -78 °C (Scheme 2). The resulting PTA-CO₂Li can be isolated as an air-stable,

Scheme 2



highly water-soluble (*S*_{25°} ~ 800 g/L) off-white solid and exhibits a ³¹P{¹H} NMR resonance at -88.0 ppm (s). In addition to water, PTA-CO₂Li is soluble in methanol, ethanol, and DMSO. A solid-state IR spectrum obtained for PTA-CO₂Li contains the expected absorbances at 1614 and 1399 cm⁻¹ for the asymmetric and symmetric C-O stretches, respectively. Isotopically labeled PTA-¹³CO₂Li was synthesized from ¹³CO₂ (vide infra) resulting in shifts in the IR stretching modes to 1592 and 1371 cm⁻¹ for the asymmetric and symmetric modes, respectively. The observed IR shifts of 22–28 cm⁻¹ are slightly less than the 36 cm⁻¹ predicted from a simple Hooke’s law calculation due to coupling of the two vibrational modes.

We have also synthesized PTA-CO₂Li without organic solvent, utilizing a heterogeneous solid/gas reaction of CO₂(g) with powdered PTA-Li in a cold bath.³⁷ Compared with the reaction in THF, the neat CO₂(g) reaction is not as clean, resulting in two resonances in the ³¹P{¹H} NMR spectrum of PTA-CO₂Li (-88.4 and -87.4 ppm). The minor product at -87.4 ppm varies in yield from 5 to 45% of the total product. In an effort to determine the nature of these two products, we synthesized PTA-¹³CO₂Li, utilizing ¹³CO₂. The ³¹P NMR spectrum of PTA-¹³CO₂Li in CD₃OD is similar to that of the unenriched product, containing two resonances: a doublet at -90.8 ppm (²*J*_{PC} = 7.6 Hz) and a triplet at -93.4 ppm (²*J*_{PC} = 9.5 Hz). In D₂O, the triplet was observed further downfield than the doublet at -87.4 ppm (*t*, ²*J*_{PC} = 8.8 Hz) and -88.4 ppm (d, ²*J*_{PC} = 7.6 Hz). The carbonyl region of the ¹³C{¹H} NMR spectrum of PTA-¹³-CO₂Li in CD₃OD contained two doublets at 175.5 ppm (²*J*_{PC} = 7.4 Hz) and 174.2 ppm (²*J*_{PC} = 9.75 Hz). From the coupling constants, we determined that the resonance at 175.5 ppm in the ¹³C NMR spectrum corresponds to the ³¹P{¹H} NMR resonance at -90.8 ppm (²*J*_{PC} = 7.4 Hz). The doublet at 174.2 ppm in the ¹³C{¹H} NMR spectrum correlates with the triplet at -93.4 ppm observed in the ³¹P{¹H} NMR spectrum of PTA-¹³CO₂Li. Together, these data suggest that the second product observed in the ³¹P and ¹³C NMR spectra is the dicarboxylated product PTA-(CO₂Li)₂.

Mass spectrometry data was also obtained on both the PTA-¹³CO₂Li and PTA-CO₂Li samples. Notable peaks include [PTA-¹³CO₂]⁻ (*m/z* 201.17) and the comparable [PTA-CO₂]⁻ anion at (*m/z* 200.17). Also seen in the spectra are the dicarboxylate species: [PTA-(¹³CO₂)₂Li]⁻ and [PTA-(CO₂)₂Li]⁻ at *m/z* 252.25 and 250.18, respectively.

The esterification of PTA-CO₂Li was accomplished by the addition of Me₃SiCl to a methanol solution of the carboxylate (Scheme 3).³⁸ The product is soluble in water, acetone, THF, diethyl ether, chloroform, methylene chloride, and acetonitrile. A shift in the ³¹P{¹H} NMR spectrum of

(37) See the Supporting Information for more details.

Scheme 3

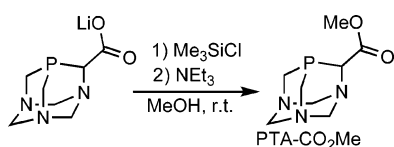


Table 2. $^{31}\text{P}\{^1\text{H}\}$ NMR and Solubility Data for the Series of PTA-CRR'OH, PTA-CO₂Li, and PTA-CO₂CH₃ Compounds; Phosphine Oxide Chemical Shift in Parentheses

	$^{31}\text{P}\{^1\text{H}\}$ NMR	S°_{25} (g/L)
PTA ^{1,34}	-98.3 ^b (-2.49)	235
PTA-CRR'OH		
R = C ₆ H ₅ , R' = C ₆ H ₅	-95.5 ^a (-3.46)	5.9
R = C ₆ H ₄ OMe, R' = C ₆ H ₄ OMe	-96.4 ^a (-3.1)	10.6
R = C ₆ H ₄ OMe, R' = H	-102.6 ^a (-1.48)	11.1
R = ferrocenyl, R' = H	-105.7 ^a (-3.19)	11.1
	-100.6 ^a (-0.06)	3.9
	-103.1 ^a (-1.35)	3.9
PTA-CO ₂ Li	-88.0 ^b (-0.91)	~800
PTA-CO ₂ Me	-93.7 ^c (-11.0)	^d

^a In CDCl₃. ^b In D₂O. ^c In CD₃OD. ^d Not determined.

PTA-CO₂Me (-93.7 ppm in D₂O) relative to PTA (-98.3 in D₂O) and PTA-CO₂Li (-88.0 ppm in D₂O) was observed (Table 2). The ¹H NMR spectrum of PTA-CO₂Me is very similar to that of PTA-CO₂Li with the exception of the singlet at 3.76 ppm representing the methyl ester. Likewise, in the ¹³C NMR spectrum the methoxy group appears as a singlet at 51.5 ppm. The ¹³C NMR resonances for the carbons in the cage are shifted significantly from those of the parent PTA ligand. The methylene carbons on the "upper rim" of PTA can be found at 50.3 ppm (d, $J_{\text{PC}} = 21$ Hz); PTA-CO₂Me possesses three resonances for the upper rim carbons of PTA-CO₂Me, 60.1 (d, $J_{\text{PC}} = 25.4$ Hz) 50.2 (d, $J_{\text{PC}} = 21.6$ Hz) and 47.2 (d, $J_{\text{PC}} = 24.6$ Hz). The "lower rim" carbons, which are now chemically inequivalent, appear as a singlet and two doublets at 74.6 (s), 72.5 (d, $^3J_{\text{PC}} = 2.2$ Hz), and 67.9 (d, $^3J_{\text{PC}} = 3.0$ Hz). The carbonyl carbon is observed as a doublet at 170.3 ppm (d, $^2J_{\text{PC}} = 8.9$ Hz).³⁷

Structure of O=PTA-CO₂Me. PTA-CO₂Me is stable in the solid state, but somewhat air-sensitive in solution. Crystals of PTA-CO₂Me grown over the course of a few days afford crystals of the oxide O=PTA-CO₂CH₃. The solid-state structure of O=PTA-CO₂CH₃ was determined by X-ray crystallography (Figure 2). Similar to the PTA-PPh₂ and other upper rim PTA derivatives described herein, the P1-C1 bond length is slightly elongated at 1.834(4) Å relative to that of the adjacent methylenes (P1-C2 = 1.815(4), P1-C3 = 1.818(4) Å).

Addition to Aldehydes and Ketones. The synthesis of β-phosphino alcohols has been accomplished through the insertion of ketones or aldehydes into the C-Li bond of PTA-Li. The reaction proceeds cleanly in moderate to good yield (>60% isolated yield) for aryl aldehydes and ketones. Addition to aliphatic ketones and aldehydes is slightly more complex, presumably due to the acidic nature of the C-H

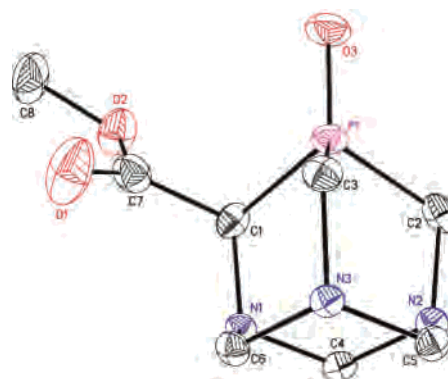
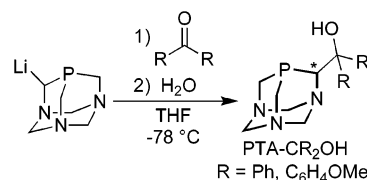
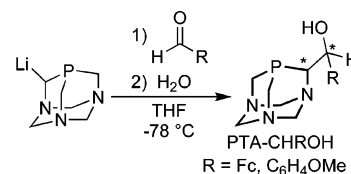


Figure 2. Thermal ellipsoid representation (50% probability) of O=PTA-CO₂CH₃ with the atomic numbering scheme. Only the R enantiomer is shown; however, both the R and S enantiomers are present in the structure. Selected bond lengths (Å) and angles (deg): P1-O3 = 1.483(3); P1-C1 = 1.834(4); P1-C2 = 1.815(4); P1-C3 = 1.818(4); C7-O1 = 1.219(5); C1-N1 = 1.484(5); C1-C7 = 1.491(5); P1-C1-C7 = 110.2(3); C7-C1-N1 = 116.6(3).

Scheme 4



Scheme 5



bond(s) adjacent to the carbonyl functionality.³⁹ Nucleophilic addition of PTA-Li to an aldehyde or ketone formally results in an alkoxide, which has not been isolated due to issues associated with separation from residual PTA—an omnipresent side product in reactions with PTA-Li. Quenching the product with H₂O allows for the isolation and purification of the β-phosphino alcohols. The reaction of PTA-Li with symmetric ketones results in a racemic mixture of products; the single chiral center in the PTA-Li starting material renders it chiral and racemic (Scheme 4). Both benzophenone and *p*-methoxybenzophenone react cleanly and easily with PTA-Li, and single resonances are observed in the ³¹P NMR spectra of the resulting products (Table 2). The ¹H NMR spectra of the products are not first order and thus very complicated due to unusual coupling patterns and the close proximity of many of the chemical shifts.

Unlike ketones, which result in enantiomeric products, the addition to aldehydes leads to PTA-CHR(OH) ligands with two contiguous chiral centers and, therefore, diastereomeric mixtures of products (Scheme 5). The ¹H NMR spectra of the PTA-CHROH compounds are even more complicated than the analogous PTA-CR₂OH ligands, as each spectrum provides data on diastereomeric compounds. The ³¹P{¹H} NMR spectrum of PTA-CH(C₆H₄OCH₃)OH contains two

(38) (a) Nakao, R.; Oka, K.; Fukumoto, T. *Bull. Chem. Soc. Jpn.* **1981**, *54*, 1267–1268. (b) Brook, M. A.; Chan, T. H. *Synthesis* **1983**, *3*, 201–203.

(39) Wong, G. W.; Frost, B. J., unpublished results.

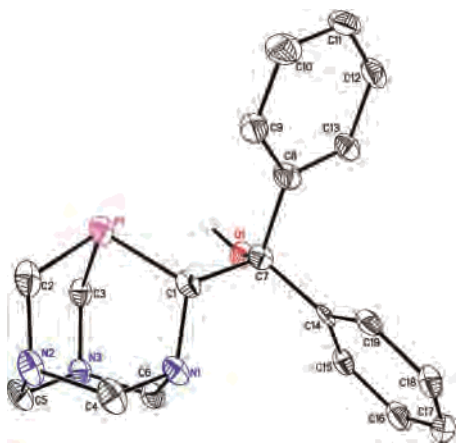


Figure 3. Thermal ellipsoid representation (50% probability) of PTA–C(C₆H₅)₂OH with the atomic numbering scheme. Only the R enantiomer is shown; however, both the R and S enantiomers are present in the structure. Hydrogen atoms have been omitted for clarity. Selected bond lengths (Å) and angles (deg): P1–C1 = 1.880(4); P1–C2 = 1.871(5); P1–C3 = 1.864(4); C7–O1 = 1.435(5); C1–N1 = 1.494(5); C1–C7 = 1.523(6); P1–C1–C7 = 112.8(3); C7–C1–N1 = 114.9(3); C8–C7–C14 = 109.5(3).

singlets at -102.6 and -105.7 ppm, one for each diastereomer. The ferrocenyl derivative, PTA–CH(ferrocenyl)OH, exhibits two ^{31}P NMR resonances at -100.6 and -103.1 ppm. Some diastereoselectivity is observed in the synthesis of the products as we isolate PTA–CH(C₆H₄OCH₃)OH as a 2.5:1 mixture of diastereomers and PTA–CH(ferrocenyl)OH as a 1.8:1 mixture of diastereomers.

The parent PTA ligand is highly water-soluble with $S_{25}^{\circ} = 235$ g/L;^{1,34} PTA–CO₂Li is 3–4 times more soluble in water and $S_{25}^{\circ} \approx 800$ g/L (vide supra). The PTA–CRR'OH ligands are soluble in water ($S_{25}^{\circ} = 3.9$ – 11.1 g/L); however, they are much less soluble than PTA (Table 2).

The solid-state structures of PTA–C(C₆H₅)₂OH, O=PTA–C(C₆H₄OCH₃)₂OH, O=PTA–CH(C₆H₄OCH₃)OH, and PTA–CH(ferrocenyl)OH were determined by X-ray crystallography. Figures 3–6 contain thermal ellipsoid representations of each compound along with selected bond lengths and angles. As seen with other upper rim PTA derivatives (PTA–PPh₂³² and O=PTA–CO₂CH₃), P1–C1 is slightly elongated with respect to the other P–CH₂ bonds due to the addition of the substituent. Derivatives of PTA substituted at the upper rim are air-stable in the solid state; in solution they oxidize over the course of days (vide supra).³² Crystals of PTA–C(C₆H₄CH₃)₂OH and PTA–CH(C₆H₄CH₃)OH grown over the course of a week resulted in X-ray-quality crystals of the phosphine oxides (Figures 4 and 5). X-ray-quality crystals of PTA–C(C₆H₅)₂OH and PTA–CH(ferrocenyl)OH were grown with careful exclusion of oxygen (Figures 3 and 6). All four structures contain both enantiomers: R/S for O=PTA–C(C₆H₄OCH₃)₂OH and PTA–C(C₆H₅)₂OH and R-S/S-R for O=PTA–CH(C₆H₄OCH₃)OH and PTA–CH(ferrocenyl)OH.

Ruthenium Complexes. Dyson and others have reported that ruthenium arene complexes of PTA and PTA derivatives, (η^6 -arene)RuX₂PTA, show anticancer activity.^{3–13} A library of compounds has been explored through substitutions to the arene and X fragments.^{5,9} Due to the small number of PTA derivatives available, only a limited number of substitu-

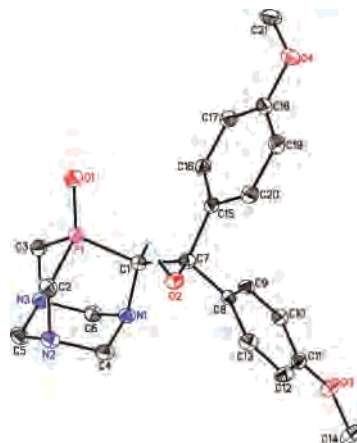


Figure 4. Thermal ellipsoid representation (50% probability) of O=PTA–C(C₆H₄OCH₃)₂OH with the atomic numbering scheme. Only the S enantiomer is shown; however, both the R and S enantiomers are present in the structure. Hydrogen atoms have been omitted for clarity. Selected bond lengths (Å) and angles (deg): P1–O1 = 1.4926(14); P1–C1 = 1.838(2); P1–C2 = 1.822(2); P1–C3 = 1.817(2); C7–O2 = 1.425(2); C1–N1 = 1.490(2); C1–C7 = 1.562(3); P1–C1–C7 = 117.61(13); C7–C1–N1 = 112.75(15).

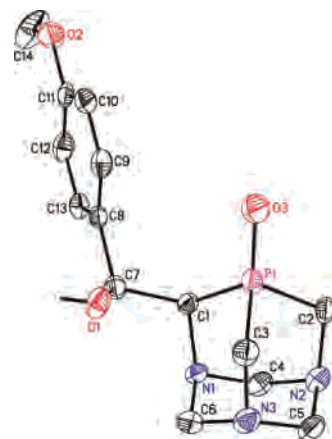


Figure 5. Thermal ellipsoid representation (50% probability) of O=PTA–CH(C₆H₄OCH₃)OH with the atomic numbering scheme. Only the R(C1)/S(C7) enantiomer is shown; however, both R(C1)/S(C7) and S(C1)/R(C7) are present in the structure. Hydrogen atoms have been omitted for clarity. Selected bond lengths (Å) and angles (deg): P1–O3 = 1.478(3); P1–C1 = 1.832(4); P1–C2 = 1.815(4); P1–C3 = 1.815(3); C7–O1 = 1.419(4); C1–N1 = 1.492(4); C1–C7 = 1.536(5); P1–C1–C7 = 117.5(3); C7–C1–N1 = 111.4(3).

tions have been made thus far to the PTA fragment. The synthesis of various PTA derivatives described herein, via the electrophile insertion into PTA–Li, offers the opportunity to develop a large library of PTA derivatives in a minimal time frame. We have synthesized three such ruthenium arene derivatives with our new chiral phosphines.

The synthesis of (η^6 -arene)RuCl₂(PTA–CRR'OH) complexes was accomplished in moderate to good yield by addition of PTA–CRR'OH to a solution of [Ru(η^6 -arene)Cl₂]₂ in CH₂Cl₂ (Scheme 6). These complexes have exhibited modest water solubility, 5.4 g/L for (η^6 -C₆H₅CH₃)RuCl₂(PTA–C(C₆H₅)₂OH) and a slightly more soluble 14.1 g/mL for (η^6 -C₆H₆)RuCl₂(PTA–C(C₆H₅OCH₃)₂OH). The compounds were characterized by NMR spectroscopy and X-ray crystallography. The $^{31}\text{P}\{^1\text{H}\}$ NMR spectra of (η^6 -C₆H₆)RuCl₂(PTA–C(C₆H₅OCH₃)₂OH) and (η^6 -C₆H₅CH₃)RuCl₂(PTA–C(C₆H₅)₂OH) contain a single resonance at -31.3 and

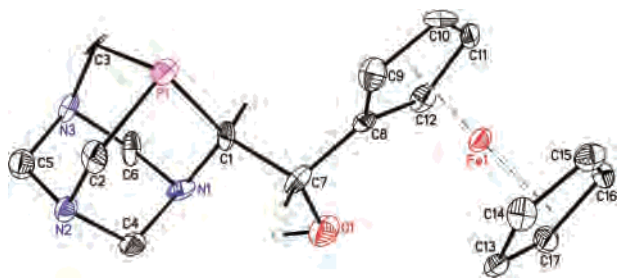


Figure 6. Thermal ellipsoid representation (50% probability) of PTA-CH(ferrocenyl)OH with the atomic numbering scheme. Only the S(C1)/R(C7) enantiomer is shown; however, both R(C1)/S(C7) and S(C1)/R(C7) are present in the structure. Hydrogen atoms have been omitted for clarity. Selected bond lengths (Å) and angles (deg): P1-C1 = 1.867(7); P1-C2 = 1.867(7); P1-C3 = 1.868(7); C7-O1 = 1.443(7); C1-N1 = 1.469(8); C1-C7 = 1.555(8); P1-C1-C7 = 115.4(5); C7-C1-N1 = 109.3(5).

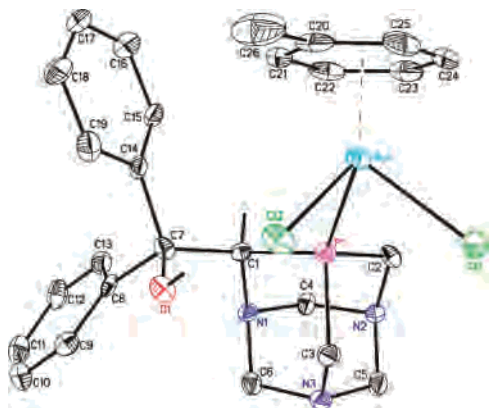
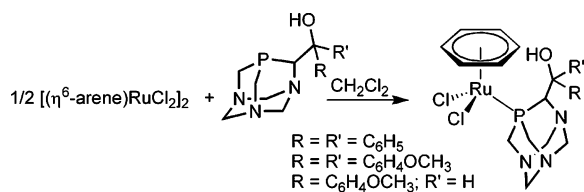


Figure 7. Thermal ellipsoid representation (50% probability) of $[(\eta^6\text{-C}_6\text{H}_5\text{-CH}_3)\text{Ru}(\text{PTA-C}(\text{C}_6\text{H}_5)_2\text{OH})\text{Cl}_2]$ with the atomic numbering scheme. The R enantiomer is shown here, but both R and S are present in the structure. Hydrogen atoms have been omitted for clarity. Selected bond lengths (Å) and angles (deg): Ru1-P1 = 2.3294(11); Ru1-C11 = 2.4119(12); Ru1-Cl2 = 2.4077(12); Ru1-arene_{cent} = 1.694; C7-O1 = 1.416(5); P1-Ru1-C11 = 83.76(4); P1-Ru1-Cl2 = 84.63(4); C11-Ru1-Cl2 = 88.79(4).

Scheme 6



−31.0 ppm, respectively. The diastomeric compound $(\eta^6\text{-C}_6\text{H}_6)\text{RuCl}_2(\text{PTA-CH}(\text{C}_6\text{H}_5\text{OCH}_3)\text{OH})$ contains two $^{31}\text{P}\{^1\text{H}\}$ chemical shifts for the two possible stereoisomers at −33.1 and −32.3 ppm for the major and minor diastomer, respectively.

The structures of three ruthenium arene complexes were determined, with each containing a PTA-CRR'OH ligand bound in a κ^1 binding mode wherein the phosphorus is bound to the metal center. Figures 7–9 contain thermal ellipsoid representations of three $(\eta^6\text{-arene})\text{RuCl}_2(\text{PTA-CRR'OH})$ complexes along with selected bond lengths and angles.

The ligands we have described should be capable of chelating to metal centers upon deprotonation of the alcohol functionality. Attempts to deprotonate the ligand and enforce a chelating κ^2 P,O or N,O binding mode were promising.⁴⁰ Upon the addition of either CsCO_3 or NaOH , a shift in the

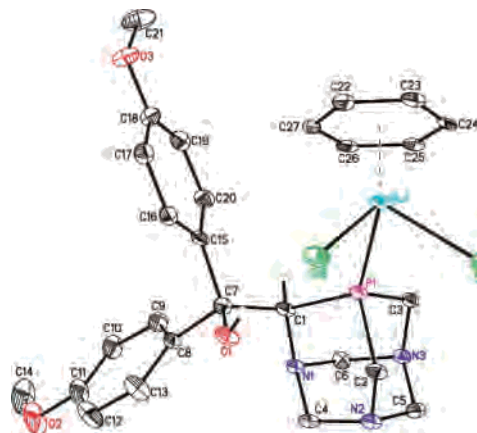


Figure 8. Thermal ellipsoid representation (50% probability) of $[(\eta^6\text{-C}_6\text{H}_6)\text{Ru}(\text{PTA-C}(\text{C}_6\text{H}_4\text{OCH}_3)_2\text{OH})\text{Cl}_2]$ with the atomic numbering scheme. Only the R enantiomer is shown; however, both enantiomers are present in the structure. Hydrogen atoms have been omitted for clarity. Selected bond lengths (Å) and angles (deg): Ru1-P1 = 2.3255(11); Ru1-C11 = 2.4343(10); Ru1-Cl2 = 2.4184(11); Ru1-arene_{cent} = 1.692; C7-O1 = 1.428(5); P1-Ru1-C11 = 85.76(4); P1-Ru1-Cl2 = 85.89(4); C11-Ru1-Cl2 = 87.66(4).

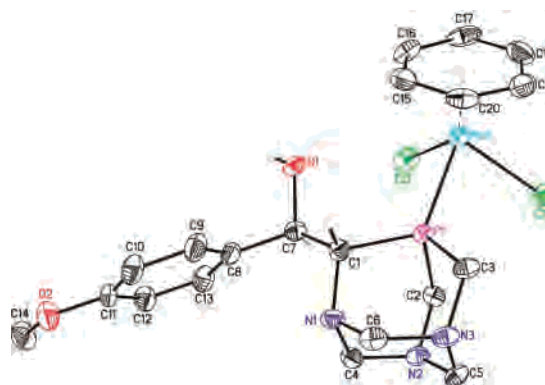


Figure 9. Thermal ellipsoid representation (50% probability) of $[(\eta^6\text{-C}_6\text{H}_6)\text{Ru}(\text{PTA-CH}(\text{C}_6\text{H}_4\text{OCH}_3)\text{OH})\text{Cl}_2]$ with the atomic numbering scheme. Only the S(C1)/R(C7) enantiomer is shown; however, both R(C1)/S(C7) and S(C1)/R(C7) are present in the structure. Selected bond lengths (Å) and angles (deg): Ru1-P1 = 2.3108(15); Ru1-C11 = 2.4122(14); Ru1-Cl2 = 2.4229(16); Ru1-arene_{cent} = 1.704; C7-O1 = 1.446(7); P1-Ru1-C11 = 82.70(5); P1-Ru1-Cl2 = 84.41(5); C11-Ru1-Cl2 = 89.00(6).

$^{31}\text{P}\{^1\text{H}\}$ resonance of $\sim 8\text{--}10$ ppm was observed. For example, the $^{31}\text{P}\{^1\text{H}\}$ resonance for $(\eta^6\text{-C}_6\text{H}_6)\text{RuCl}_2(\text{PTA-C}(\text{C}_6\text{H}_5\text{OCH}_3)_2\text{OH})$ shifted from −31 to −23 ppm upon the addition of base. Similar shifts were observed for $(\eta^6\text{-C}_6\text{H}_6)\text{RuCl}_2(\text{PTA-CH}(\text{C}_6\text{H}_5\text{OCH}_3)\text{OH})$, where a resonance at −24.55 has been observed and attributed to a chelating P,O bound ligand. Attempts to isolate and characterize the metal complexes with chelating ligands have, thus far, been unsuccessful.

Conclusion

We have reported the addition of PTA-Li to CO_2 , ketones, and aldehydes. These chiral upper-rim derivatives of PTA provide some of the benefits of the parent ligand, namely, that they are air-stable and somewhat water soluble. In

(40) We have obtained a preliminary crystal structure of a complex in which PTA-CH(ferrocenyl)O[−] is bound to one ruthenium center in a κ^2 N,O binding mode and the phosphorus atom is bound to a second ruthenium arene center. See the Supporting Information for further details.

solution, the ligands oxidize slowly over the course of days to weeks. All the ligands synthesized herein have the potential to bind metals in a κ^2 (P,O or N,O) binding mode, although only the κ^1 -P mode was observed in this report. We are currently working on separating the ligand enantiomers for use in asymmetric catalysis and for the synthesis of enantio-enriched Ru complexes.

Acknowledgment. Acknowledgment is made to the National Science Foundation CAREER program (CHE-0645365) and the donors of the American Chemical Society Petroleum Research Fund (PRF 43574-G3) for support.

G.W.W. acknowledges the McNair's Scholars program, NSF-EPSCoR (0447416), and the UNR Office of Undergraduate Research for funding. Support from the NSF is also acknowledged for the X-ray and NMR facilities (CHE-0226402 and CHE-0521191). The authors would also like to thank Drs. S. Cummings and R. Huang for their assistance.

Supporting Information Available: Detailed experimental procedures, crystallographic details, and NMR spectra of all compounds. This material is available free of charge via the Internet at <http://pubs.acs.org>.

IC701936X